Polymer Bulletin 27, 487–494 (1992)

Polymer Bulletin

Microemulsion polymerization in the water, aerosol-OT, tetrahydrofurfuryl methacrylate system

J. Texter[1], L. E. Oppenheimer[1], and J. R. Minter[2]

[1]Photographic Research Laboratories, Eastman Kodak Company, Rochester, NY 14650-2109, USA
[2]Analytical Technology Division, Eastman Kodak Company, Rochester, NY 14652-3712, USA

Summary

Part of the phase diagram at low (<10%) oil content and 25° C has been mapped in the water, Aerosol-OT (AOT), tetrahydrofurfuryl methacrylate (THFM) ternary system. Sodium persulfate/sodium metabisulfite was used as a redox initiator to induce polymerization in this microemulsion system at 7.8% (w/w) THFM and 4.4% AOT. Conversions in excess of 90% were obtained. The parent microemulsion droplets have diameters on the order of 5 nm. The resulting latexes have average particle diameters of 37-39 nm. The latex particles are cross-linked as a result of radical induced opening of the tetrahydrofurfuryl ring, and exhibit nearly the same density (1.216 g/cm^3) and glass transition temperature (67° C) as material (1.222 g/cm^3; 62° C) produced by solution polymerization. This *three-component* microemulsion, and the corresponding latexes, have been imaged directly by cryo-electron microscopy. The first reports of three-component polymerized (oil in water) microemulsions, stabilized by *cationic* surfactants, were made by Murtagh, Ferrick, and Thomas [*ACS Polymer Preprints* **1987**, *28*, 441] and more recently by Perez-Luna, Puig, Castano, Rodriguez, Murthy, and Kaler [*Langmuir* **1990**, *6*, 1040]. This report appears to be the first such polymerization in a three-component system stabilized with an *anionic* surfactant. These latexes are cross-linked beads, and are the first such examples to be prepared by microemulsion polymerization.

Introduction

Microemulsion polymerization as an alternate means of creating latexes and foams from polymerizable monomers is now over a decade old(1-23), but is still an emerging technology. Microemulsions containing continuous and discontinuous domains generally have droplet diameters significantly less than 10 nm. The possibility of imparting kinetic stability to such nanosized particles, after spontaneous microemulsification, is a principal driving force in the development of this polymerization technology. Such goals have already been widely met in the case of water-in-oil microemulsions containing acrylamide, as has been extensively demonstrated by Candau and her collaborators(4,8,11,12,15,18,19,24). Similar successes may be expected to obtain for water pools containing other water soluble monomers. The production of nano-latexes from *oil-in-water* microemulsions of monomers has not as yet become routine. Very small microemulsions can be obtained for such systems, although their polymerization generally results in latexes 20-80 nm in diameter(4,7,14,16,21-23). Particle size control in such systems remains an area of interest and opportunity.

The first polymerization in a *three-component* (oil in water) microemulsion was reported by Murtagh et al.(16) for styrene swollen cetyltrimethylammonium bromide (CTAB)

micelles. Particle sizes ranged from 11 to 56 nm, depending on the amount of initiator added. More recently, Perez-Luna et al.(21) reported the polymerization in much more concentrated microemulsions of styrene, dodecyltrimethylammonium bromide (DTAB), and water at 60° C. They estimated their parent microemulsion particles to have diameters on the order of 16-26 nm (14% DTAB; 4-8% styrene). The resulting monodisperse latexes, however were somewhat larger (20-31 nm in diameter). Most recently, Vinson et al. (25) have suggested that *dilute* CTAB(1%)/styrene(0.6%)/water microemulsions could be polymerized at 27° C to produce 8-9 nm diameter latex particles *20% smaller than the parent droplets.*

In this report we examine microemulsion polymerization in the three-component Aerosol-OT (AOT), tetrahydrofurfuryl methacrylate (THFM), water system at 25° C. Poly(THFM) has found application in use as a component in paint-on artificial finger nails(26) and in low-shrinkage dental and biomedical materials(27-30). THFM has also found useful application in the formulation of copolymeric loadable-latexes, since the tetrahydrofurfuryl group imparts a significant degree of solubilizing power to copolymers with respect to the imbibition of photographically useful compounds that are relatively hydrophobic and insoluble in aqueous solution(31).

Experimental

Materials

AOT (bis[2-ethylhexyl]sulfosuccinate sodium salt) was obtained from Fluka and used as received. THFM was obtained from Sartomer and used as received for mapping the phase diagram. Methylether hydroquinone (MEHQ), added to the THFM as a preservative,was removed prior to polymerization by passing THFM through a DHR-4 column (Specialty Polymer Products). Sodium persulfate and sodium metabisulfite, used as initiators, were obtained from J. T. Baker and Aldrich respectively.

Polymerization

The parent microemulsion, approximately 114 g, was prepared in a 250 ml roundbottomed flask and stirred continuously with a magnetic stirring bar at 25° C. The microemulsion was sparged for 40 min with nitrogen, before addition of an aqueous initiator cocktail (26.5 mℓ). Sodium persulfate, at 1% (w/w) of THFM, and sodium metabisulfite, at 0.25% (latex *A*) or at 0.005% (latex *B*), were added as redox initiators. Thereafter a nitrogen blanket was kept over the microemulsion; the nitrogen was humidified by passing it through a water trap before use in the reaction flask. After a reaction period of 22-28 h, the turbid reaction mixture was washed with distilled water in an Amicon membrane filtration system to remove excess surfactant and unreacted monomer. Reaction extent was determined by gas chromatographic (GC) analysis of the latex suspension and of the aqueous filtrate. The same procedure was used to determine the amount of AOT.

Bulk poly(THFM) was prepared according to the methods of Zafar and Mahmud(32) by two methods. In one case the sample was prepared using neat THFM. In the other case, polymerization was done in methylbenzoate solution. A 60° C water bath was used to maintain temperature for 8-10 g samples placed in test tubes. Samples for thermal analysis were obtained ultimately by freezing chunks of polymer in liquid nitrogen, and pulverizing the resulting glass in a mortar and pestle. The fine powder obtained was heated in a vacuum oven

for 60 h at 75-80 ° C to remove remaining unreacted monomer or solvent (methyl benzoate).

Quasi-Elastic Light Scattering

All scattering measurments were done using a thermostated sample cell, surrounded by toluene, at 25° C. The latex suspensions were filtered through Millipore Millex®-SR 0.2-μm filter units prior to measurement. Anotop 25 0.2-μm filters were used to filter the parent microemulsion prior to measurement. Photocorrelation measurements were done with a Brookhaven Instruments BI 240 goniometer and BI 2030 correlator (128 channel). An Innova 90-4 argon ion laser (Coherent Radiation) operating at 514.5 nm was used as a light source for the microemulsion samples. A Melles-Griot HeNe laser (model 05-LHP-171) operating at 632.8 nm was used as a light source for the latex samples. Measurements were performed over the angular range of 30° to 135° in 15° increments. Cumulant analysis was used to calculate the decay constant, Γ, of the correlation function for each measurement. The apparent diffusion coefficient at each concentration was then obtained by linear least-squares analysis of the dependence of Γ on q^2 (33). The scattering vector q is given by

$$q = 4\pi\ n \sin(\theta/2)/\lambda$$

where n is the solvent refractive index and λ is the wavelength of the incident light in vacuum. The linear dependence was valid throughout the range measured in the case of the latexes and valid for $\theta > 75°$ in the case of the parent microemulsion. The apparent diffusion coefficients obtained from the slopes at each concentration were plotted as a function of concentration, and the infinite dilution value of the diffusion coefficient was obtained by extrapolation. The Stokes-Einstein equation was used to convert the apparent diffusion coefficient, D, to a hydrodynamic diameter by

$$d = kT/3\pi\eta D$$

where η is the viscosity of the continuous phase.

Cryo-Electron Microscopy

Direct images of vitrified thin films of the parent and polymerized microemeulsions were recorded at -175° C in a Philips CM-12 transmission electron microscope equipped with a Gatan Model 626 cryotransfer holder. Thin liquid films were prepared at 100% relative humidity and 25° C within a controlled environmental vitrification system (CEVS) similar to the one described by Bellare et al.(34). A 7-$\mu\ell$ droplet of microemulsion was placed on a carbon coated cellulose acetate butyrate film containing holes 8-10 μm in diameter(35). Most of the fluid was removed from the grid by blotting with filter paper. This blotting resulted in the formation of thin, biconcave menisci of fluid spanning the holes in the grid. The controlled environment of the CEVS prevented loss of volatile species from the film. Immediately after cessation of blotting, a shutter in the bottom of the CEVS was opened and the tweezers containing the specimen were plunged into liquid ethane just above its freezing point. The cooling rate in these thin films is sufficient to prevent crystallization of water, resulting in a vitreous sample. Each grid was transferred to liquid nitrogen for storage until it was transferred to the Gatan 626 holder and inserted into the electron microscope for imaging. The specimen temperatures never exceed -160° C during the process, well below the devitrification temperature of water, -140° C (36).

Thermal Analysis

Differential scanning calorimetry was done using a Du Pont/TA Instruments DSC 910 operated in a heat flux, rather than power compensation mode. Heating rates were 10° C/min

in a nitrogen stream (30 cc/min). Glass transition temperatures (Tg) were obtained by heating over the -25° C to 100° C interval, and quenching between heating cycles. Transitions measured during *second* and *third* heating cycles were taken as indications of Tg. Sample measurements were done using hermetically sealed pans and by using pans not sealed hermetically. Thermal (decomposition) gravimetric analysis (TGA) was studied using a Perken-Elmer TGS-II thermal gravimetric analyzer. Nitrogen at 60 cc/min was used as a carrier gas, and the heating rate was 10° C/min.

Results and Discussion

Phase Diagram

The phase diagram at 25° C was mapped by titrating with THFM along *x*% AOT (in water) tie-lines (*x* = 0, 0.5, 1, 2, 3, 4, 5, and 6). The isotropic single-phase microemulsion region, L_1, is illustrated in Fig. 1. This region is bounded on either side by two-phase regions. To the left of this isotropic region is the L_1+D region, consisting of lamellar liquid crystalline (D) and micellar (L_1) components. The boundary between the L_1 and L_1+D regions on the 0% THFM axis is approximately at 1.4% AOT(37,38). The isotropic THFM phase (L_2) boundary on the 0% AOT axis with the L_1 region is approximately at 0.5% THFM. To the right of the L_1 phase and above the 0% AOT axis, we have a two-phase L_1+L_2 region. The cross in Fig. 1 corresponds to the formulation used in the polymerizations (after addition of the initiator cocktail); this point corresponds to 7.8% THFM and 4.4% AOT. This corner of the phase diagram is similar to that reported(38) for the water/AOT/*p*-xylene system.

Microemulsions of this formulation are quite transparent to the eye. We attempted to determine the approximate particle size by QELS. Samples formulated *without* removing the preservative (MEHQ) and *with* 4 mM aqueous sodium sulfate (to simulate electroylte effects of initiator) were used for the scattering (and TEM) experiments. The corresponding decay constant as a function of the square of the scattering vector, *q*, for scattering angles 90°, 105°, 120°, and 135° are illustrated in Fig. 2. A linear least squares fit of this data indicates an approximate particle diameter of 9.2 nm. This estimate is only approximate, because the corresponding particle-particle interaction and correlation parts of the scattering problem (39) were not deconvoluted in this treatment. *Retardation* of particle motion by repulsive particle-particle interactions generally leads to overestimations of size by QELS.

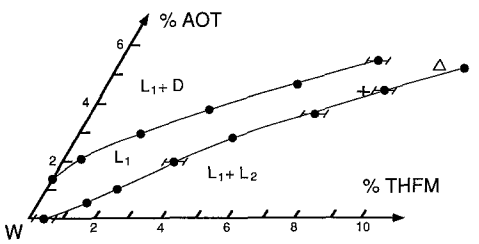

Fig. 1. Partial ternary phase diagram at 25° C. The cross indicates where microemulsion polymerization was started. The triangle indicates the formulation before initiator addition.

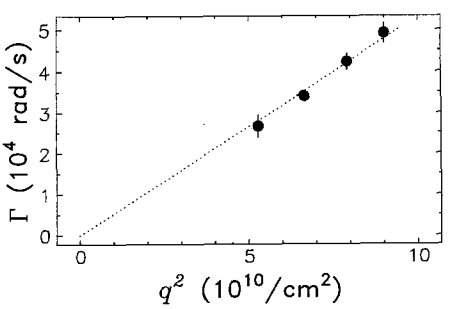

Fig. 2. QELS for the microemulsion formulated at the point indicated by the cross in Fig. 1.

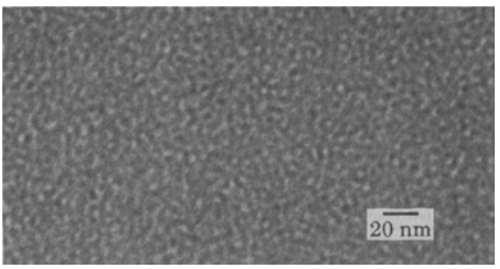

Fig. 3. TEM of the parent microemulsion, sampled at the position indicated with a cross in Fig. 1.

Direct TEM images of the parent microemulsion (Fig. 3) reveal a swollen micellar morphology similar to that observed in other oil-water-surfactant systems(25,40). The films are sufficiently thick that the projection is not as clear as in the case of other micellar systems(25). Vinson et al.(25) were the first to report *direct* TEM imaging of microemulsions (swollen micelles) of 1% CTAB and 0.4% toluene or 0.6% styrene. It is noteworthy that our microemulsion, at 12.2% THFM+AOT, is an order of magnitude more concentrated than those imaged by Vinson et al. The size of these THFM+AOT microemulsion particles appears, at about 5 nm, significantly smaller than the 9.2 nm suggested by the QELS data of Fig. 2, and smaller than the 6-10 nm diameter swollen micelles imaged by Vinson et al.(25).

Polymerization and Characterization

The microemulsions for polymerization were initially formulated at the Δ-point indicated in the phase diagram (Fig. 1; 9.5% THFM, 5.4% AOT). Addition of the initiator cocktail (17.2 mM sodium persulfate and 5.4 mM [latex *A*] *or* 0.11 mM [latex *B*] sodium metabisulfite; in 26.5 mℓ) moved the point of polymerization initiation to the position indicated by the cross in Fig. 1. After 22 (*A*) and 28 (*B*) h of reaction, the now turbid latex suspensions were washed with distilled water (55 [*A*] and 108 [*B*] turnovers) to remove excess surfactant and unreacted monomer. GC analysis of the latex suspensions and the filtrate volumes for THFM indicated conversions of 94% (*A*) and 90% (*B*) were obtained for the two latexes.

QELS analyses of these latexes, as a function of wt%, are illustrated in Fig. 4, where the zero-intercept extrapolations indicate particle sizes on the order of 64 (*A*) and 73 nm (*B*) were obtained. TEM images of these latexes are illustrated in Fig. 5 and indicate that the actual particle sizes are on average considerably *smaller* than these estimates obtained by QELS.

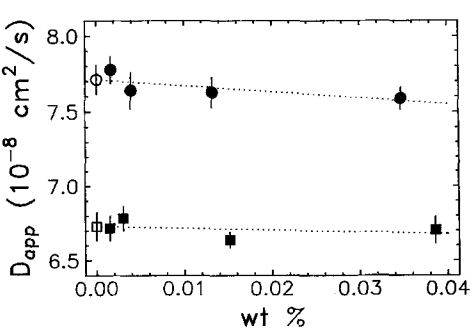

Fig. 4. Apparent diffusion coefficients of the latex particles determined by QELS as a function of concentration. The upper curve (•) corresponds to initiation with the high level of metabisulfite, and has a zero-concentration intercept (○) of 7.71±0.05 x 10^{-8} cm^2/s (d ≈ 64±2 nm). The lower curve (■) corresponds to initiation with the low level of metabisulfite, and has a zero-concentration intercept (□) of 6.73±0.05 x 10^{-8} cm^2/s (d ≈ 73±3 nm).

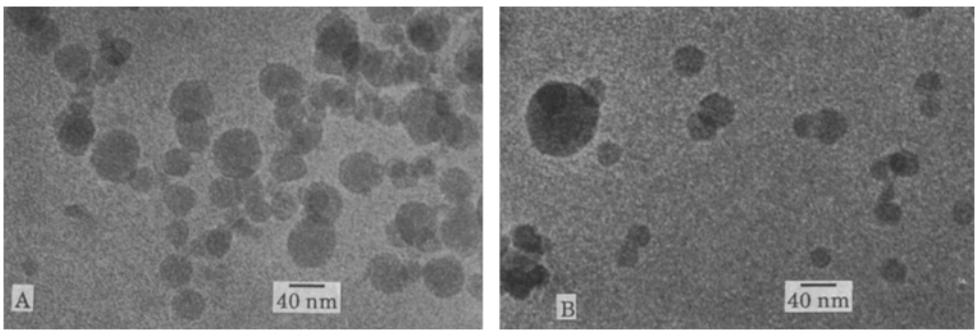

Fig. 5. Transmission electron micrographs (TEM) of the two latex samples, (*A*) high metabisulfite in the initiator and (*B*) low metabisulfite in the initiator. These TEM were obtained by cryogenic vitrification as described in the text.

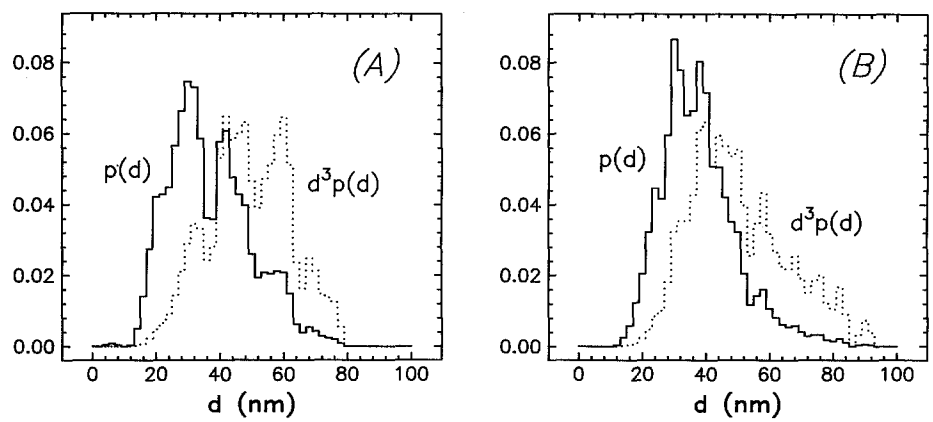

Fig. 6. Particle size distributions for the product latexes obtained by image analysis of TEM. Distributions for the latexes with high (*A*) and low (*B*) levels of metabisulfite in the initiator are shown. The number-frequency distributions, *p(d)* (————), and the normalized volume-weighted distributions, $d^3p(d)$ (· · · · · ·), are illustrated.

Image analysis of numerous fields obtained by TEM was used to generate the particle size distributions illustrated in Fig. 6, where mean particle diamters of 37 (*A*) and 39 nm (*B*) were obtained from the resulting number-frequency distributions, *p(d)*. These two distributions are statistically indistinguishable. The turbidity of these latexes comes from the relatively small fraction of large (60-90 nm) particles present in each sample. The impact of these larger fractions is illustrated in Fig. 6 where normalized volume-weighted distributions, $d^3p(d)$ are also shown. These larger particles also dominate the QELS measurements. The respective *p(d)* are not monodisperse. The breadths of these distributions may be due to the proximity of the polymerization initiation point to the boundary of the isotropic single-phase region (Fig. 1), or due to the lengthy polymerization time and low temperature (slow kinetics) of the polymerization. There was not a significant driving force for locking-in the initial droplet size of the parent microemulsion.

Density gradient centrifugation indicated the latex particles had densities of 1.215±0.003 (*A*) and 1.217±0.003 (*B*) g/cm^3; these values are not significantly different. A slightly higher

value of 1.222 g/cm^3 has been reported(30) for poly(THFM) produced by solution polymerization. Thermal analysis of the dried latexes indicated glass transition temperatures (Tg) of 68° ±2° C in non-hermetically sealed pans and 65° ± 1° C in hermetically sealed pans for *A* and *B*. The slightly lower value in the hermetically sealed pans is consistent with slight plasticization by a small amount of retained monomer. These Tg are considerably higher than the 47° C reported by Patel et al.(29) for poly(THFM). Patel et al., however, used a heating rate of 2° C/min (we used 10° C/min), and they did not specify pretreatment and heating cycle details. We therefore prepared samples by solution polymerization *neat* and in methyl benzoate solution for comparison with our latexes. We found these samples were very sensitive to pretreatment conditions, and exhibited Tg over the range of 36° - 66° C, depending on pretreatment and which heating cycle was used for measurement. Our pulverization and heat treatment of these bulk samples yielded Tg of 64° ± 1° C in non-hermetically sealed pans and 60° ±2° C in hermetically sealed pans. These values are in reasonably close agreement with the values obtained for the latexes.

Attempts to determine molecular weight distributions for the poly(THFM) in the latexes failed, because polymer obtained as dried latex could not be dissolved in any common solvent, including THF. This insolubility can be attributed to cross-linking identified by Patel and Braden(30). The chain polymerization causes ring-opening in the tetrahydrofurfuryl group(30). The resulting radical is free to react with another such fragment or another vinyl group. These microemulsion polymerized latexes therefore constitute cross-linked beads. The DSC analyses of the latexes were driven past 100° C to 200° C during the third and final heating cycle. An *exotherm* commenced generally at about 100° C and peaked in the range of 130° - 170° C, well below the onset of thermal decomposition at 250° C (determined by TGA). This exotherm can reasonably be assigned to driving further cross-linking between pendent groups, and will be examined more closely in a subsequent report.

Acknowledgements

The authors would like to thank Robert J. Meyer, for assistance in electron microscopy, Roger Moody and Patty Sciotti, for assistance in executing the DSC and thermogravimetric analyses, Tim Schmandt, for assistance in the sedimentation centrifugation determinations of density, and Skip Wolcott, for assistance in the GC determination of AOT and THFM. The preparation of the manuscript benefited from critical suggestions and comments by David D. Miller and Eric W. Kaler.

References

1. Stoffer JO, Bone T (1980) *J Polym Sci: Polym Chem* **18**: 2641.
2. Stoffer JO, Bone T (1980) *J Dispersion Sci Technol* **1**: 37.
3. Atik SS, Thomas JK (1982) *J Am Chem Soc* **104**: 5868.
4. Leong YS, Candau F (1982) *J Phys Chem* **86**: 2269.
5. Atik SS, Thomas JK (1983) *J Am Chem Soc* **105**: 4515.
6. Gan LM, Chew CH, Friberg SE (1983) *J Macromol Sci-Chem* **A19**:739.
7. Tang H-I, Johnson PL, Gulari E (1984) *Polymer* **25**: 1367.
8. Candau F, Leong YS, Pouyet G, Candau S (1984) *J Colloid Interface Sci* **101**: 167.
9. Johnson PL, Gulari E (1984) *J Polym Sci: Polym Chem* **22**: 3967.
10. Jayakrishnan A, Shah DO (1984) *J Polym Sci: Polym Letters* **22**: 31.
11. Candau F, Leong YS, Fitch RM (1985) *J Polym Sci: Polym Chem* **23**: 193.

12. Candau F, Zekhnini Z, Durand J-P (1986) *J Colloid Interface Sci* **114**: 398.
13. Grätzel CE, Jirousek M, Grätzel M (1986) *Langmuir* **2**: 292.
14. Kuo P-L, Turro NJ, Tseng C-M, El-Asser MS, Vanderhoff JW *Macromol* **20**: 1216.
15. Candau F, Zekhnini Z, Durand J (1987) *Progr Colloid Polymer Sci* **73**: 33.
16. Murtagh J, Ferrick MR, Tomas JK (1987) *ACS Polym Preprints* **28**: 441.
17. Haque E, Qutubuddin S (1988) *J Polym Sci: Part C: Polym Letters* **26**: 429.
18. Carver MT, Dreyer, Knoesel R, Candau F, Fitch RM (1989) *J Polym Sci: PArt A: Polym Chem* **27**: 2161.
19. Carver MT, Candau F, Fitch RM (1989) *J Polym Sci: Part A: Polym Chem* **27**: *2179.*
20. Dunn AS (1989) Polymerization in Micelles and Microemulsions. In: Eastmond GC, Ledwith A, Russo S, Sigwalt P (eds.) *Comprehensive Polymer Science. The Synthesis, Characterization, Reactions & Applications of Polymers. Vol. 4. Chain Polymerization II.* Pergamon, London, pp 219-224.
21. Perez-Luna VH, Puig JE, Castano VM, Rodriguez BE, Murthy AK, Kaler EW (1990) *Langmuir* **6**: 1040.
22. Puig JE, Corona-Galvan S, Maldonado A, Schulz P, Rodriguez BE, Kaler EW (1990) *J Colloid Interface Sci* **137**: 308.
23. Gan LM, Chew CH, Lye I, Imae T *Polym Bull* **25**: 193.
24. Candau F (1989) Polymerization in Micelles and Microemulsions. In: Eastmond GC, Ledwith A, Russo S, Sigwalt P (eds.) *Comprehensive Polymer Science. The Synthesis, Characterization, Reactions & Applications of Polymers. Vol. 4. Chain Polymerization II.* Pergamon, London, pp 225-229.
25. Vinson PK, Bellare JR, Davis HT, Miller WG, Scriven LE (1991) *J Colloid Interface Sci* **142**: 74.
26. Fuller M. (1982) *J Soc Cosmet Chem* **33**: 51.
27. Bhusate M, Braden M. (1983) *UK Patent Application* GB 2,107,341A.
28. Lee H, Colby C. (1986) *Dental Mater* **2**: 175.
29. Patel MP, Braden M, Davy KWM (1988) *Biomaterials* **8**: 53.
30. Patel MP, Braden M (1989) *Biomaterials* **10**: 277.
31. Upson DA, Steklenski DJ (1985) *US Patent* 4,544,723.
32. Zafar MM, Mahmud R. (1974) *Makromol Chem* **175**: 2627.
33. Koppel DE (1972) *J Chem Phys* **57**: 4814.
34. Bellare JR, Davies HT, Scriven LE, Talmon Y. (1988) *J Electron Microsc Tech* **10**: 87.
35. Fukami A, Adachi K (1965) *J Electron Microscopy* **14**: 112.
36. Dubochet J, Lepault J, Freeman R, Berriman JA, Homo J-C (1982) *J Microsc* **128**: 219.
37. Rogers J, Winsor PA (1968) *Nature (London)* **216**: 477.
38. Ekwall P, Mandell L, Fontell K (1970) *J Colloid Interface Sci* **33**: 215.
39. Chang NJ, Kaler EW (1986) *Langmuir* **2**: 184.
40. Vinson PK *Cryo-electron Microscopy of Microstructures in Complex Liquids*, Thesis, University of Minnesota, Minneapolis, Minnesota, 1990.

Accepted December 4, 1991 K